

## Bayesian Search of Massive Scalar Fields from LIGO-Virgo-KAGRA Binaries

Yiqi Xie<sup>1</sup>, Adrian Ka-Wai Chung<sup>1</sup>, Thomas P. Sotiriou<sup>2,3</sup> and Nicolás Yunes<sup>1</sup>

<sup>1</sup>*Illinois Center for Advanced Studies of the Universe, Department of Physics, University of Illinois at Urbana-Champaign, Urbana, Illinois 61801, USA*

<sup>2</sup>*Nottingham Centre of Gravity, University of Nottingham, University Park, Nottingham, NG7 2RD, United Kingdom*

<sup>3</sup>*School of Mathematical Sciences & School of Physics and Astronomy, University of Nottingham, University Park, Nottingham, NG7 2RD, United Kingdom*



(Received 23 October 2024; accepted 9 April 2025; published 16 May 2025)

Massive scalar fields are promising candidates for addressing many unresolved problems in fundamental physics. We report the first model-agnostic Bayesian search of massive scalar fields that are nonminimally coupled to gravity in LIGO/Virgo/KAGRA gravitational-wave data. We find no evidence for such fields and place the most stringent upper limits on their coupling for scalar masses  $\lesssim 2 \times 10^{-12}$  eV. We exemplify the strength of these bounds by applying them to massive scalar-Gauss-Bonnet gravity, finding the tightest constraints on the coupling constant to date,  $\sqrt{\alpha_{\text{GB}}} \lesssim 1$  km for scalar masses  $\lesssim 10^{-13}$  eV to 90% credible level.

DOI: [10.1103/PhysRevLett.134.191402](https://doi.org/10.1103/PhysRevLett.134.191402)

**Introduction**—Scalar fields are ubiquitous in extensions of general relativity (GR) or the Standard Model of particle physics [1–6], motivated by the quest for quantum gravity and attempts to address internal consistency problems, e.g. hierarchy problem [7], strong *CP* problem [8]. Light scalars have also been suggested as potential explanations for dark energy [9] or dark matter [10,11].

The inspiral behavior of compact binaries can be significantly affected if a scalar endows compact stars or black holes (BHs) with a scalar monopole, making gravitational waves (GWs) a promising probe of new fundamental scalars. Such a binary would emit scalar dipolar radiation, in addition to the standard quadrupole gravitational radiation. The extra loss of energy would affect the orbital dynamics and, in turn, the conventional gravitational-wave polarizations, leading to a GW dephasing that is  $\mathcal{O}(v^2/c^2)$  larger than the leading-order term in the GR GW phase, where  $v$  is the orbital velocity and  $c$  is the speed of light [i.e., a  $-1$  post-Newtonian (PN) order effect] [12–14]. Thus, the effect of the additional dipolar emission on the orbital dynamics is very significant in the early inspiral phase. Indeed, pulsar observations have all but ruled out the prospect that compact stars could carry a scalar charge if the scalar field is massless [15,16]. LIGO-Virgo-KAGRA (LVK) observations have been used to search for scalar fields with black hole binaries [17–26],

while future observations of highly asymmetric binaries by the Laser Interferometer Space Antenna (LISA) have been shown to have great potential as well [27–29].

Searches for massive scalars with GW present an additional challenge: massive fields are confined near the compact objects and this suppresses scalar emission in the early inspiral. Indeed, GW observations are likely “blind” to fields whose inverse mass is smaller than the size of the compact objects of the binary. Nonetheless, axion-like particles are expected to be very light but not massless [1,3,11], while deviations from GR that lead to interesting non-linear strong field phenomena, such as scalarization [30–35], include massive scalars. Indeed, the GW signal emitted by a binary neutron star (binary NS, or BNS), the GW170817 event, was analyzed for a model-specific search of axion at a discrete grid of axion mass in [36]. A model-agnostic search for massive scalar fields was explored in [37] through Fisher analysis using a simulated, synthetic dataset. Both analyses were done for some particular values of the scalar field mass only.

In this work, we report the first model-agnostic Bayesian search of massive scalar fields from GW signals detected by the LVK detectors during their first three observing runs (O1–O3) [38–43] as well as the latest one released in O4 [44], without fixing the scalar mass  $\mu_s \hbar$  *a priori*. This analysis is agnostic to the theory that endows the binary component with a scalar charge. We find no evidence for dipolar emission in BH binaries (BNSs) for scalar masses  $\mu_s \hbar \lesssim 5 \times 10^{-13}$  eV ( $2 \times 10^{-12}$  eV). In a more focused range  $\mu_s \hbar \lesssim 3 \times 10^{-13}$  eV, we show constraints on the difference in the scalar charge per unit mass in BH binaries (BNSs) to be  $\lesssim 0.5$  (0.05). These are the first and most stringent Bayesian GW constraints on these massive scalar

Published by the American Physical Society under the terms of the [Creative Commons Attribution 4.0 International license](https://creativecommons.org/licenses/by/4.0/). Further distribution of this work must maintain attribution to the author(s) and the published article’s title, journal citation, and DOI.

fields in this mass range. We note that dipole radiation is a generic feature and a smoking-gun effect of nonminimally coupled scalars on compact binaries, see, e.g., [45] for an example given in massive Brans-Dicke theory.

We also repeat our analysis for a specific massive scalar-tensor theory, massive scalar-Gauss-Bonnet (massive sGB, or msGB) gravity. In geometric units  $G = 1 = c$ , the msGB action writes

$$S = \int d^4x \sqrt{-g} \left[ \frac{R}{16\pi} + \alpha_{\text{GB}} \varphi \mathcal{X}_{\text{GB}}^2 - \frac{1}{2} (\nabla_a \varphi \nabla^a \varphi + \mu_s^2 \varphi^2) \right] + S_{\text{matter}}, \quad (1)$$

where  $g$  is the determinant of the metric  $g_{ab}$ ,  $R$  is the Ricci scalar,  $\varphi$  is a real scalar field with mass  $\mu_s \hbar$ ,  $S_{\text{matter}}$  is the matter action,  $\mathcal{X}_{\text{GB}}^2 = R^2 - 4R_{ab}R^{ab} + R_{abcd}R^{abcd}$  is the Gauss-Bonnet (GB) invariant,  $R_{ab}$  and  $R_{abcd}$  are the Ricci tensor and the Riemann tensor, respectively, and  $\alpha_{\text{GB}}$  is a dimensionful coupling constant. We here obtain the first Bayesian LVK constraints on  $\sqrt{\alpha_{\text{GB}}}$  for a massive scalar, with 90% credible intervals  $\lesssim 1$  km for scalar masses  $\lesssim 10^{-13}$  eV.

Massive sGB provides a rather minimal model for scalar hair from a massive field in BH binaries, and yet it is sufficiently general for inspiral modeling. The linear coupling between  $\varphi$  and  $\mathcal{X}_{\text{GB}}^2$  included in our action is the only shift-symmetric term that can evade no-hair theorems [46–48] and lead to scalar hair [49–52]. More general couplings with  $\mathcal{X}_{\text{GB}}^2$ , couplings with other curvature invariants, or self-coupling of the scalar, could exhibit broader phenomenology in general (e.g., [31–35]), but are expected to be subdominant in our setup and can be thus modeled perturbatively. A nonzero  $\mu_s$  would be expected if such additional interactions break shift-symmetry, and it could also arise from non-perturbative instanton effects [53]. Hence, we consider massive sGB a fairly representative model for our analysis.

*Dipole emission from massive scalar fields*—BHs with scalar hair in the  $\mu_s = 0$  case of the action in Eq. (1) have been studied extensively [49–51,54]. The scalar asymptotes to  $\varphi_{\text{BH}}(r) = Q_{\text{BH}}/r$ , where  $r$  is the radial coordinate and  $Q_{\text{BH}}$  is the scalar charge. At the leading order in  $\alpha_{\text{GB}}$  [24,55,56],

$$Q_{\text{BH}} = \frac{\sqrt{16\pi}\alpha_{\text{GB}}}{m} \frac{2\sqrt{1-\chi^2}}{1+\sqrt{1-\chi^2}}, \quad (2)$$

where  $m$  and  $\chi$  are the mass and the dimensionless spin of the BH, respectively. For  $\mu_s > 0$ , there is an additional Yukawa-like suppression of the scalar field at large distances, and the asymptotic field profile takes the form  $\varphi_{\text{BH}}(r) = Q_{\text{BH}} e^{-\mu_s r}/r$ . Here, we approximate  $Q_{\text{BH}}$  endowed by the massive field with Eq. (2), which is valid

because GW observations only allow for small  $\mu_s$  values to be searched over (see [57] for further discussion of scalar hair in msGB). Note that a linear coupling between a scalar and the GB invariant does not endow neutron stars (NSs) with a scalar monopole [58], and hence, hereafter we take  $Q_{\text{NS}} = 0$ .

When at least one of the two compact objects in a binary carries scalar charge there will be dipolar emission but it will only kick in when the orbital angular frequency,  $\Omega$ , reaches the Compton angular frequency of the scalar field. Indeed, for quasicircular orbits, the dipole radiation power from a generic massive scalar field has been solved in [14,59],

$$\delta\dot{E} = -\frac{1}{3}\eta^2 M^2 \Omega^4 r_{12}^2 |\Delta\tilde{Q}|^2 \left(1 - \frac{\mu_s^2}{\Omega^2}\right)^{3/2}, \quad (3)$$

where subscripts 1,2 denote the primary and secondary component of the binary,  $\Delta\tilde{Q} = Q_1/m_1 - Q_2/m_2$  is a dimensionless dipole parameter,  $M = m_1 + m_2$  is the total mass,  $\eta = m_1 m_2 / M^2$  is the symmetric mass ratio,  $r_{12}$  is the orbital separation.

The change of radiation power in Eq. (3) can be mapped to the inspiral waveform using the parametrized post-Einsteinian framework [60,61] (see Supplemental Material [62] for details). We focus here on the dominant (2,2) harmonic, as others are related through a simple scaling [63–65]. In the frequency domain, the modified waveform can be written as

$$\tilde{h}(f) = \tilde{h}_{\text{GR}}(f) e^{-i\delta\Psi(f)}, \quad (4)$$

where  $f = \Omega/\pi$  is the GW frequency,  $\tilde{h}_{\text{GR}}$  is a GR waveform, which we here choose from the IMRPhenom family (e.g., [66–72]), and  $\delta\Psi$  describes the correction to GR. At a stage where the dipole has been activated but the binary is far from merging, the correction is

$$\delta\Psi(f) \sim -\frac{5|\Delta\tilde{Q}|^2}{7168\eta(\pi M f)^{7/3}}, \quad f_{\text{act}} < f < f_{\text{insp}}, \quad (5)$$

up to a linear function of  $f$ , where  $f_{\text{act}} = \mu_s/\pi$  is the dipole activation frequency and  $f_{\text{insp}} = 0.018/M$  is an estimated ending frequency of the inspiral. Beyond the frequency range prescribed above, we apply no physical modification but only linearly extrapolate Eq. (5) to satisfy the requirement of  $C^1$  continuity. We neglect corrections from the change in the binary's binding energy as, for a massive field, these would affect higher PN orders only [14].

*Gravitational wave parameter estimation*—We use LVK open data [43,73] and focus on specific events selected for the LVK parametrized inspiral tests of GR [84–86], each of which is (i) detected by at least two detectors, (ii) has a false-alarm rate less than  $10^{-3}$  yr $^{-1}$ , and (iii) accumulates an SNR greater than 6 during the inspiral. We further filter

the list with the requirement that either  $M < 30M_\odot$  or there is strong evidence of mass asymmetry by the LVK analysis [74–76], as a smaller  $M$  elongates the inspiral, while, according to Eq. (5), the same dipole  $|\Delta\tilde{Q}|$  leads to a greater GR deviation when  $M$  and  $\eta$  are smaller. We also add the latest O4 event, GW230529 [44], for the msGB analysis since several works before us [20–22] have claimed the tightest constraint on massless sGB gravity using this event. This leaves us with 16 events (see Supplemental Material [62] for a full list).

For each event, we perform Bayesian parameter estimation with the waveform model of Eqs. (4) and (5) and a Gaussian noise model. The  $\tilde{h}_{\text{GR}}$  function in Eq. (4) is taken to be IMRPhenomPv2 [66–68] for symmetric BH binaries and IMRPhenomPv2\_NRTidalv2 [72] for BNSs. For asymmetric binaries or NSBH candidates, we choose  $\tilde{h}_{\text{GR}}$  to be IMRPhenomXPHM [69–71] with an additional (3,3) mode that reasonably covers higher-multipole contributions [74–76].

Exploiting the Bilby inference library [87] with the dynesty nested sampler [88], we estimate the posterior distribution for  $\vec{\lambda}_{\text{GR}} \cup \{\mu_s, |\Delta\tilde{Q}| \text{ or } \sqrt{\alpha_{\text{GB}}}\}$ , where  $\vec{\lambda}_{\text{GR}}$  are source parameters, such as binary masses and spins, which  $\tilde{h}_{\text{GR}}$  depends on. The posterior is then marginalized over  $\vec{\lambda}_{\text{GR}}$  and smoothed with a method based on Gaussian kernel density estimation. We extract the 90% bounds for  $|\Delta\tilde{Q}|$  and  $\sqrt{\alpha_{\text{GB}}}$  as functions of  $\mu_s$  when constraining a generic massive dipole and msGB gravity, respectively. In the latter case, the waveform is reparametrized with Eq. (2), and a combined 90% bound is also obtained by multiplying the likelihoods from the single-event analysis.

Because NSs do not acquire scalar charges in sGB gravity, we only analyze BNSs when constraining a generic massive dipole. The source of GW190814 may either be a binary BH or an NSBH [75]. The former case would result in a tighter sGB constraint because then  $|\Delta\tilde{Q}|$  would be dominated by  $\alpha_{\text{GB}}/m_s^2$ , where  $m_s$  is the smaller mass in the binary that carries a scalar charge; the dipole effect is smaller for NSBHs because  $m_s$  has to take the larger, primary (BH) mass value. Here, we assume GW190814 is an NSBH to obtain a conservative msGB constraint. The source of GW230529 is an NS and an object of unknown nature (most likely a BH) [44]. Following [20–22], we analyze this event as an NSBH, but we do not include it in the combined msGB analysis.

Our waveform model assumes that the modification to GR is small so we must check that this is respected by our posteriors. In [18,19],  $\sqrt{\alpha_{\text{GB}}}/m_s < 0.5$  is proposed as a validity cutoff in *massless* sGB theory. We will not try to enforce this condition, or attempt to generalize it here, as the  $\mu_s > 0$  case is fundamentally different. Since dipolar emission effectively kicks in at a certain frequency, one can have virtually zero deviations from GR for parts of the waveform, even for large couplings, while deviations could

still be significant in the later inspiral. Hence, we will instead require

$$\mathcal{N}_e(\delta\Psi)/\mathcal{N}_e(\Psi_{\text{GR}}^{\text{OPN}}) < 1, \quad (6)$$

where  $\Psi_{\text{GR}}^{\text{OPN}}$  is the leading-PN-order GR phase, while

$$\mathcal{N}_e(\Psi) = \min_{\phi,t} \left[ \int \frac{df |\tilde{h}(f)|^2 (\Psi(f) + \phi + 2\pi ft)^2}{4\pi^2 \text{SNR}^2 S_n(f)} \right]^{1/2}, \quad (7)$$

are *effective cycles* [89], which measure the number of GW cycles incurred by  $\Psi$ , as weighted by a noise spectral density  $S_n$ . According to condition (6), the validity cutoff for  $\sqrt{\alpha_{\text{GB}}}$  (or  $|\Delta\tilde{Q}|$ ) increases with  $\mu_s$ , because the frequency range of modifications in  $\delta\Psi$  is smaller when  $\mu_s$  is larger.

Given Eq. (5), when  $\mu_s > \pi f_{\text{insp}}$ , there is no modification to GR, and a constraint on the dipole is not possible. In the Supplemental Material [62], we show that the likelihood does not die out fast enough as  $|\Delta\tilde{Q}| \rightarrow \infty$ , but rather it asymptotes to the GR likelihood multiplied by a factor equal to the GR posterior probability of  $f_{\text{insp}} < \mu_s/\pi$ . We refer to the latter as the “fraction of indifference” (FOI) and only report the 90% bounds in the range  $\text{FOI}(\mu_s) < 1\%$ , where the GR posterior for computing the FOI is estimated with a separate nested sampling run under the same computational settings. For the combined msGB constraint, we multiply the FOIs in alignment with the multiplication of single-event likelihoods.

The priors used in our analysis are uniform over  $|\Delta\tilde{Q}| \in [0, 1]$  and  $\sqrt{\alpha_{\text{GB}}} \in [0, 10]$  km, except that for GW230529 the  $\sqrt{\alpha_{\text{GB}}}$  prior is limited within  $[0, 1]$  km to avoid unphysical results falsely supported by the single-detector data [21]. The prior over  $\mu_s$  is uniform in a logarithmic scale, between  $f_{\text{act}} = \mu_s/\pi = 10$  Hz and a  $\mu_s$  value sufficiently beyond the FOI limit. The lower bound of  $\mu_s$  can be treated in the same way as in the  $\mu_s \rightarrow 0$  limit because the LVK data has a lower frequency cutoff at 20 Hz and it is blind to any activation before that. The prior choice for  $\vec{\lambda}_{\text{GR}}$  is adapted from the LVK standard analysis assuming GR [39–42,77], and combines electromagnetic observations when available [78–82]. After running parameter estimation, we find 3 events showing posterior artifacts that are irrelevant to the massive scalar field of interest, and we exclude these events from results (both single-event and combined) presented hereafter. See Supplemental Material [62] for a full list of  $\vec{\lambda}_{\text{GR}}$  and their priors, the detailed settings and postprocessing for each sampling run, the posterior results of each event, and discussion of the posterior artifacts.

*Constraints on dipole emission from massive scalars*—In Fig. 1(a), we show the single-event constraints on  $|\Delta\tilde{Q}|$  for generic dipole emission. A black dotted curve is additionally drawn for the lowest validity cutoff across all O1–O3

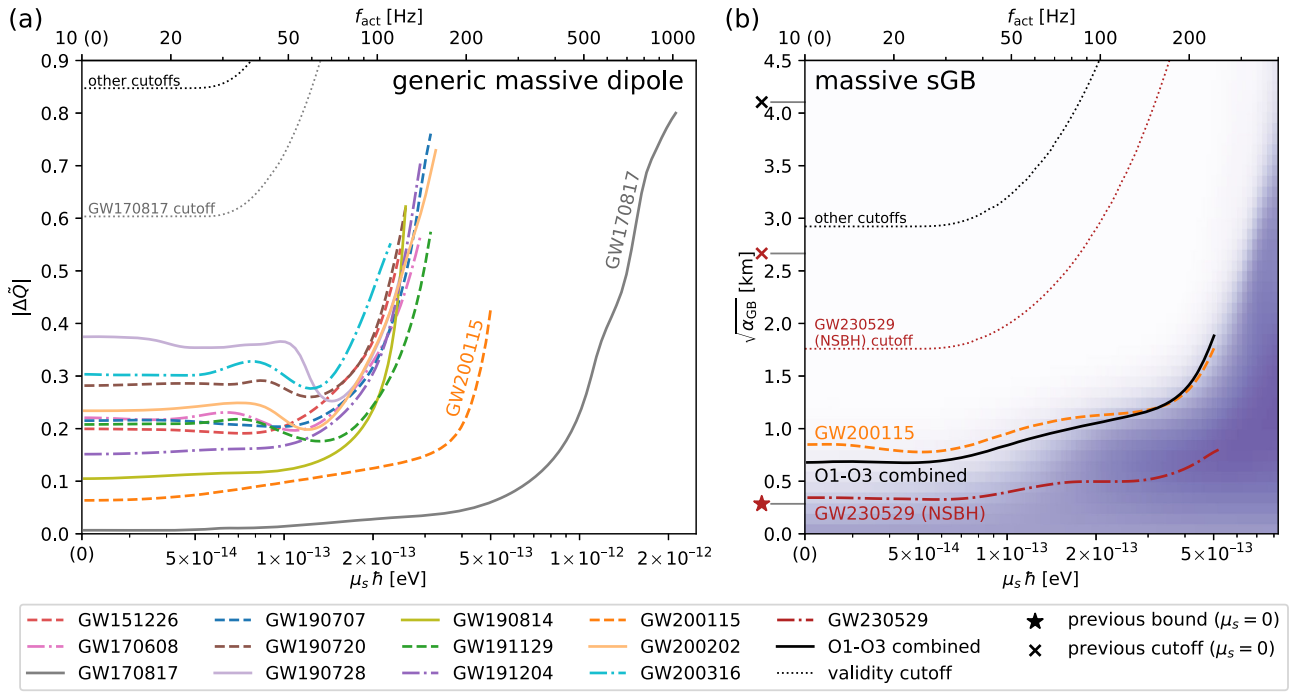


FIG. 1. Constraints on dipole emission from massive scalar fields. Panel (a) shows the 90% bound on the dimensionless dipole parameter  $|\Delta\tilde{Q}|$  as a function of the scalar mass  $\mu_s$  for each O1–O3 binary. Panel (b) shows the same as (a), but for the sGB coupling constant  $\sqrt{\alpha_{\text{GB}}}$  in msGB gravity, using the GW200115 event and the combination of O1–O3 BH binaries (accompanied by the combined 2D posterior shaded in purple). Panel (b) is also overlaid with the bound from the O4 event GW230529 assuming it is an NSBH, which is not included in the combined analysis. The left end of each bound curve is equivalent to the  $\mu_s \rightarrow 0$  limit, given the lower-frequency cutoff of the data. The right end is limited by the FOI condition or the finite width of the  $|\Delta\tilde{Q}|$  or  $\sqrt{\alpha_{\text{GB}}}$  prior [GW170817 in panel (a) and GW230529 in panel (b)]. The dotted curves show the validity cutoffs for specific binaries, while “other cutoffs” refer to the lowest one across O1–O3 BH binaries. Each star (cross) marks the center of previous 90% bounds [20–22] for massless sGB (consistent with a  $\sqrt{\alpha_{\text{GB}}}/m_s < 0.5$  cutoff [18,19]), with different colors indicating different binaries, i.e. crimson for GW230529 and black for “others” combined.

BH binaries, and we confirm that every 90% bound from such a binary is below this curve (and hence also below each one’s own validity cutoff). The same also applies to the GW170817 and GW230529 constraints, for which the validity cutoffs are significantly lower and are plotted separately. As previously discussed, the constraint becomes weaker and is eventually entirely lifted as  $f_{\text{act}} = \mu_s/\pi$  approaches and surpasses  $f_{\text{insp}}$ , where we stop reporting the 90% bound based on the FOI condition. For GW170817 and GW230529, however, we observe a saturation of the prior before the FOI limit, so we only show the range in which the posterior 90% bound is below 80% of the prior maximum. Despite that, GW170817 still presents the widest constraints,  $\mu_s \hbar \lesssim 2.1 \times 10^{-12}$  eV, because it has the smallest binary total mass, and hence, it is the longest inspiral—for the same reason we also observe the most stringent dipole constraint  $|\Delta\tilde{Q}| \lesssim 0.0067$  in the  $\mu_s \rightarrow 0$  limit from GW170817.

Between the  $\mu_s \rightarrow 0$  limit and the point where  $|\Delta\tilde{Q}|$  becomes practically unconstrained, the variation of the 90% bound is nonmonotonic for each event. Sometimes, the bound on  $|\Delta\tilde{Q}|$  can at first become tighter as one moves

to larger  $\mu_s$ , before becoming looser again. This is because the sudden activation of the dipole would be better observed by the detectors as  $f_{\text{act}}$  moves toward their sensitivity buckets, near  $\mathcal{O}(10^2)$  Hz.

In Fig. 1(b), we show the combined constraint on  $\sqrt{\alpha_{\text{GB}}}$  in msGB gravity, together with the combined posterior (shaded in purple) and the best single-event constraint from GW200115 up to O3. These constraints satisfy condition (6) and  $\sqrt{\alpha_{\text{GB}}}/m_s < 0.5$  by their lowest cutoffs across all events. Because FOIs are multiplied, the combined constraint is reported up to a higher scalar mass  $\mu_s \hbar \lesssim 5.2 \times 10^{-13}$  eV, where we see the weakest 90% bound is  $\sqrt{\alpha_{\text{GB}}} \lesssim 1.88$  km. In the massless limit  $\mu_s \rightarrow 0$ , the combined 90% bound suggests  $\sqrt{\alpha_{\text{GB}}} \lesssim 0.68$  km [90]. Our results show that such a constraint (to 90% credible level) is maintained all the way up to  $\mu_s \hbar \lesssim 10^{-13}$  eV, before significantly weakening.

We have not included the O4 event GW230529 [44] in our combined analysis as it could well be a BNS, in which case the dipole emission would be suppressed [58]. However, since Refs. [20–22] have used this event to obtain tight constraints on massless sGB assuming the

source is an NSBH, we have analyzed it as a single event under the same assumption and overlaid its single-event msGB 90% bound curve on top of Fig. 1(b). In the  $\mu_s \rightarrow 0$  limit, we find  $\sqrt{\alpha_{\text{GB}}} \lesssim 0.34$  km, which is consistent with [20–22]. The full curve, therefore, shows how these results are extended to the massive regime (up to  $\mu_s \hbar \lesssim 5.2 \times 10^{-13}$  eV due to the prior edge, see Supplemental Material [62]).

*Discussion and future prospects*—We have conducted the first model-agnostic Bayesian search of massive scalar fields nonminimally coupled to gravity using LVK data and also considered a specific well-motivated theory, msGB gravity. In both cases, we find no modifications to GR, and, when the mass is below a certain threshold (set by the characteristic frequency of the binary), we obtain constraints on the scalar charge or coupling that are as stringent as those for a massless scalar, but for a wide range of masses. The constraints on the charge or coupling constant are comparable for all scalar masses below the threshold, strongly suggesting that imposing a bound on or measuring a mass below that threshold will be hard. Past that threshold, bounds on the charge or coupling weaken rapidly.

The tightest constraints from a single event come from different events in each of the two approaches. The BNS event that gives the tightest bound in the model-agnostic search is entirely absent in the msGB case, as NSs do not carry scalar monopoles in this theory. But even for BH binaries, one gets the tightest bounds from different events. In msGB, where one can meaningfully combine events, the resulting constraint is a significant improvement with respect to the tightest single-event constraints, at least for lower masses.

For lower masses, we expect the constraints we have obtained in msGB gravity to be conservative and robust to the inclusion of additional interaction terms, provided that the linear coupling between the scalar and the GB invariant is the dominant contribution to the scalar charge for stationary BHs. Additional interaction terms would then be expected to contribute at higher PN orders [91], which would be relevant only in the late inspiral.

The above discussion is based on current LVK data, but future observations of lighter binaries and longer inspirals with more advanced ground-based detectors [92–94] can progressively improve the constraints. Pushing the bounds to higher scalar masses is challenging though. As the scalar mass gets closer to the threshold beyond which the constraints on the charge rapidly weaken, the onset of dipolar emission is pushed to the late inspiral, and higher PN corrections become more relevant, in both a model-agnostic and a theory-specific approach. In addition, the baseline GR model also becomes less accurate approaching the merger. Hence, obtaining reliable bounds in that part of the parameter space will be rather challenging both technically and observationally.

Space-based detectors planned in the 2030s [95–98] will open up a new window for constraining scalar fields with extreme mass-ratio inspirals (EMRIs) [27,28,99]. Current conservative estimates suggest that detecting EMRIs with LISA would yield a bound on the order of  $Q_2/m_2 \sim 0.002$  or  $\sqrt{\alpha_{\text{GB}}} \sim 0.2$  km [29]. EMRI observations have also been shown to be able to measure or provide a bound for the scalar mass [99]. However, LISA bounds are inherently limited to lower scalar masses than LVK or 3G detectors, as they probe larger separations. An interesting prospect, if nonzero scalar charges were to be detected, is combining observations from ground-based detectors and LISA to place a bound on the mass of the scalar.

*Acknowledgments*—We thank Carl-Johan Haster, Anna Liu, Hector O. Silva, and Kent Yagi for useful discussions. Y. X., A. K. W. C., and N. Y. acknowledge support from the Simons Foundation through Award No. 896696, the NSF through Grant No. PHY-2207650 and NASA through Grant No. 80NSSC22K0806. Y. X. also acknowledges support from the Illinois Center for Advanced Studies of the Universe (ICASU) / Center for Astrophysical Surveys (CAPS) Graduate Fellowship. T. P. S. acknowledges partial support from the STFC Consolidated Grant No. ST/V005596/1 and No. ST/X000672/1. This work made use of the Illinois Campus Cluster, a computing resource that is operated by the Illinois Campus Cluster Program (ICCP) in conjunction with the National Center for Supercomputing Applications (NCSA), and is supported by funds from the University of Illinois Urbana–Champaign (UIUC).

- 
- [1] S. Weinberg, *Phys. Rev. Lett.* **40**, 223 (1978).
  - [2] T. Damour and A. M. Polyakov, *Nucl. Phys.* **B423**, 532 (1994).
  - [3] A. Arvanitaki, S. Dimopoulos, S. Dubovsky, N. Kaloper, and J. March-Russell, *Phys. Rev. D* **81**, 123530 (2010).
  - [4] L. Barack *et al.*, *Classical Quantum Gravity* **36**, 143001 (2019).
  - [5] E. Berti *et al.*, *Classical Quantum Gravity* **32**, 243001 (2015).
  - [6] N. Yunes, X. Siemens, and K. Yagi, arXiv:2408.05240.
  - [7] N. Arkani-Hamed, S. Dimopoulos, and G. R. Dvali, *Phys. Lett. B* **429**, 263 (1998).
  - [8] A. Hook, *Proc. Sci. TASI2018* (2019) 004 [arXiv:1812.02669].
  - [9] E. J. Copeland, M. Sami, and S. Tsujikawa, *Int. J. Mod. Phys. D* **15**, 1753 (2006).
  - [10] L. Hui, J. P. Ostriker, S. Tremaine, and E. Witten, *Phys. Rev. D* **95**, 043541 (2017).
  - [11] L. Hui, *Annu. Rev. Astron. Astrophys.* **59**, 247 (2021).
  - [12] E. Barausse, N. Yunes, and K. Chamberlain, *Phys. Rev. Lett.* **116**, 241104 (2016).
  - [13] K. Chamberlain and N. Yunes, *Phys. Rev. D* **96**, 084039 (2017).
  - [14] S. Alexander, E. McDonough, R. Sims, and N. Yunes, *Classical Quantum Gravity* **35**, 235012 (2018).

- [15] J. Antoniadis *et al.*, *Science* **340**, 6131 (2013).
- [16] D. Anderson, P. Freire, and N. Yunes, *Classical Quantum Gravity* **36**, 225009 (2019).
- [17] K. Yagi, *Phys. Rev. D* **86**, 081504(R) (2012).
- [18] R. Nair, S. Perkins, H. O. Silva, and N. Yunes, *Phys. Rev. Lett.* **123**, 191101 (2019).
- [19] S. E. Perkins, R. Nair, H. O. Silva, and N. Yunes, *Phys. Rev. D* **104**, 024060 (2021).
- [20] B. Gao, S.-P. Tang, H.-T. Wang, J. Yan, and Y.-Z. Fan, *Phys. Rev. D* **110**, 044022 (2024).
- [21] E. M. Sanger *et al.*, [arXiv:2406.03568](https://arxiv.org/abs/2406.03568).
- [22] F.-L. Julie, L. Pompili, and A. Buonanno, *Phys. Rev. D* **111**, 024016 (2025).
- [23] H.-T. Wang, S.-P. Tang, P.-C. Li, M.-Z. Han, and Y.-Z. Fan, *Phys. Rev. D* **104**, 024015 (2021).
- [24] Z. Lyu, N. Jiang, and K. Yagi, *Phys. Rev. D* **105**, 064001 (2022); **106**, 069901(E) (2022).
- [25] B. Wang, C. Shi, J.-d. Zhang, Y.-M. hu, and J. Mei, *Phys. Rev. D* **108**, 044061 (2023).
- [26] A. Saffer and K. Yagi, *Phys. Rev. D* **104**, 124052 (2021).
- [27] A. Maselli, N. Franchini, L. Gualtieri, and T. P. Sotiriou, *Phys. Rev. Lett.* **125**, 141101 (2020).
- [28] A. Maselli, N. Franchini, L. Gualtieri, T. P. Sotiriou, S. Barsanti, and P. Pani, *Nat. Astron.* **6**, 464 (2022).
- [29] L. Speri, S. Barsanti, A. Maselli, T. P. Sotiriou, N. Warburton, M. van de Meent, A. J. K. Chua, O. Burke, and J. Gair, [arXiv:2406.07607](https://arxiv.org/abs/2406.07607).
- [30] T. Damour and G. Esposito-Farese, *Phys. Rev. Lett.* **70**, 2220 (1993).
- [31] H. O. Silva, J. Sakstein, L. Gualtieri, T. P. Sotiriou, and E. Berti, *Phys. Rev. Lett.* **120**, 131104 (2018).
- [32] D. D. Doneva and S. S. Yazadjiev, *Phys. Rev. Lett.* **120**, 131103 (2018).
- [33] A. Dima, E. Barausse, N. Franchini, and T. P. Sotiriou, *Phys. Rev. Lett.* **125**, 231101 (2020).
- [34] C. A. R. Herdeiro, E. Radu, H. O. Silva, T. P. Sotiriou, and N. Yunes, *Phys. Rev. Lett.* **126**, 011103 (2021).
- [35] D. D. Doneva, F. M. Ramazanođlu, H. O. Silva, T. P. Sotiriou, and S. S. Yazadjiev, *Rev. Mod. Phys.* **96**, 015004 (2024).
- [36] J. Zhang, Z. Lyu, J. Huang, M. C. Johnson, L. Sagunski, M. Sakellariadou, and H. Yang, *Phys. Rev. Lett.* **127**, 161101 (2021).
- [37] K. Yamada, T. Narikawa, and T. Tanaka, *Prog. Theor. Exp. Phys.* **2019**, 103E01 (2019).
- [38] B. P. Abbott *et al.* (LIGO Scientific and Virgo Collaboration), *Phys. Rev. X* **6**, 041015 (2016); **8**, 039903(E) (2018).
- [39] B. P. Abbott *et al.* (LIGO Scientific and Virgo Collaborations), *Phys. Rev. X* **9**, 031040 (2019).
- [40] R. Abbott *et al.* (LIGO Scientific and Virgo Collaborations), *Phys. Rev. X* **11**, 021053 (2021).
- [41] R. Abbott *et al.* (LIGO Scientific and VIRGO Collaborations), *Phys. Rev. D* **109**, 022001 (2024).
- [42] R. Abbott *et al.* (KAGRA, VIRGO, and LIGO Scientific Collaborations), *Phys. Rev. X* **13**, 041039 (2023).
- [43] R. Abbott *et al.* (KAGRA, VIRGO, and LIGO Scientific Collaborations), *Astrophys. J. Suppl. Ser.* **267**, 29 (2023).
- [44] A. G. Abac *et al.* (LIGO Scientific, Virgo, and KAGRA Collaborations), *Astrophys. J. Lett.* **970**, L34 (2024).
- [45] J. Alsing, E. Berti, C. M. Will, and H. Zaslauer, *Phys. Rev. D* **85**, 064041 (2012).
- [46] T. P. Sotiriou and V. Faraoni, *Phys. Rev. Lett.* **108**, 081103 (2012).
- [47] L. Hui and A. Nicolis, *Phys. Rev. Lett.* **110**, 241104 (2013).
- [48] T. P. Sotiriou, *Classical Quantum Gravity* **32**, 214002 (2015).
- [49] N. Yunes and L. C. Stein, *Phys. Rev. D* **83**, 104002 (2011).
- [50] T. P. Sotiriou and S.-Y. Zhou, *Phys. Rev. Lett.* **112**, 251102 (2014).
- [51] T. P. Sotiriou and S.-Y. Zhou, *Phys. Rev. D* **90**, 124063 (2014).
- [52] D. Ayzenberg and N. Yunes, *Phys. Rev. D* **90**, 044066 (2014); **91**, 069905(E) (2015).
- [53] S. Alexander, G. Gabadadze, L. Jenks, and N. Yunes (to be published).
- [54] K. Prabhu and L. C. Stein, *Phys. Rev. D* **98**, 021503(R) (2018).
- [55] E. Berti, K. Yagi, and N. Yunes, *Gen. Relativ. Gravit.* **50**, 46 (2018).
- [56] M. Saravani and T. P. Sotiriou, *Phys. Rev. D* **99**, 124004 (2019).
- [57] I. van Gemeren, T. Hinderer, and S. Vandoren, *SciPost Phys. Core* **7**, 069 (2024).
- [58] K. Yagi, L. C. Stein, and N. Yunes, *Phys. Rev. D* **93**, 024010 (2016).
- [59] D. Krause, H. T. Kloor, and E. Fischbach, *Phys. Rev. D* **49**, 6892 (1994).
- [60] N. Yunes and F. Pretorius, *Phys. Rev. D* **80**, 122003 (2009).
- [61] N. Yunes, K. Yagi, and F. Pretorius, *Phys. Rev. D* **94**, 084002 (2016).
- [62] See Supplemental Material at <http://link.aps.org/supplemental/10.1103/PhysRevLett.134.191402>, which includes Refs. [14,24,39–44,60,61,63–83], for details about the modified gravitational waveform, GW events selected for the analysis, parameter estimation scheme and post-processing procedure, individual posterior for each GW event, and analysis of posterior artifacts that leads to exclusion of certain GW events from the discussion in the main text.
- [63] K. Chatziioannou, N. Yunes, and N. Cornish, *Phys. Rev. D* **86**, 022004 (2012); **95**, 129901(E) (2017).
- [64] S. Mezzasoma and N. Yunes, *Phys. Rev. D* **106**, 024026 (2022).
- [65] A. K. Mehta, A. Buonanno, R. Cotesta, A. Ghosh, N. Sennett, and J. Steinhoff, *Phys. Rev. D* **107**, 044020 (2023).
- [66] M. Hannam, P. Schmidt, A. Bohe, L. Haegel, S. Husa, F. Ohme, G. Pratten, and M. Purrer, *Phys. Rev. Lett.* **113**, 151101 (2014).
- [67] S. Husa, S. Khan, M. Hannam, M. Purrer, F. Ohme, X. Jimenez Forteza, and A. Bohe, *Phys. Rev. D* **93**, 044006 (2016).
- [68] S. Khan, S. Husa, M. Hannam, F. Ohme, M. Purrer, X. Jimenez Forteza, and A. Bohe, *Phys. Rev. D* **93**, 044007 (2016).
- [69] G. Pratten *et al.*, *Phys. Rev. D* **103**, 104056 (2021).
- [70] G. Pratten, S. Husa, C. Garcia-Quiros, M. Colleoni, A. Ramos-Buades, H. Estelles, and R. Jaume, *Phys. Rev. D* **102**, 064001 (2020).

- [71] C. García-Quirós, M. Colleoni, S. Husa, H. Estellés, G. Pratten, A. Ramos-Buades, M. Mateu-Lucena, and R. Jaume, *Phys. Rev. D* **102**, 064002 (2020).
- [72] T. Dietrich, A. Samajdar, S. Khan, N.K. Johnson-McDaniel, R. Dudi, and W. Tichy, *Phys. Rev. D* **100**, 044003 (2019).
- [73] R. Abbott *et al.* (LIGO Scientific and Virgo Collaborations), *SoftwareX* **13**, 100658 (2021).
- [74] R. Abbott *et al.* (LIGO Scientific and Virgo Collaborations), *Phys. Rev. D* **102**, 043015 (2020).
- [75] R. Abbott *et al.* (LIGO Scientific and Virgo Collaborations), *Astrophys. J. Lett.* **896**, L44 (2020).
- [76] R. Abbott *et al.* (LIGO Scientific, KAGRA, and VIRGO Collaborations), *Astrophys. J. Lett.* **915**, L5 (2021).
- [77] P.A.R. Ade *et al.* (Planck Collaboration), *Astron. Astrophys.* **594**, A13 (2016).
- [78] A. J. Levan *et al.*, *Astrophys. J. Lett.* **848**, L28 (2017).
- [79] J. Hjorth, A. J. Levan, N. R. Tanvir, J. D. Lyman, R. Wojtak, S. L. Schröder, I. Mandel, C. Gall, and S. H. Bruun, *Astrophys. J. Lett.* **848**, L31 (2017).
- [80] M. Soares-Santos *et al.* (DES and Dark Energy Camera GW-EM Collaborations), *Astrophys. J. Lett.* **848**, L16 (2017).
- [81] M. Cantiello *et al.*, *Astrophys. J. Lett.* **854**, L31 (2018).
- [82] B. P. Abbott *et al.* (LIGO Scientific and Virgo Collaborations), *Phys. Rev. X* **9**, 011001 (2019).
- [83] LIGO Scientific, Virgo, and KAGRA Collaborations, LVK Algorithm Library—LALSuite, Free software (GPL) (2018).
- [84] R. Abbott *et al.* (LIGO Scientific and Virgo Collaborations), *Phys. Rev. D* **103**, 122002 (2021).
- [85] R. Abbott *et al.* (LIGO Scientific, VIRGO, and KAGRA Collaborations), [arXiv:2112.06861](https://arxiv.org/abs/2112.06861).
- [86] B. P. Abbott *et al.* (LIGO Scientific and Virgo Collaborations), *Phys. Rev. Lett.* **123**, 011102 (2019).
- [87] G. Ashton *et al.*, *Astrophys. J. Suppl. Ser.* **241**, 27 (2019).
- [88] J. S. Speagle, *Mon. Not. Roy. Astron. Soc.* **493**, 3132 (2020).
- [89] L. Sampson, N. Yunes, N. Cornish, M. Ponce, E. Barausse, A. Klein, C. Palenzuela, and L. Lehner, *Phys. Rev. D* **90**, 124091 (2014).
- [90] Previous works [24,25] have reported a different 90% bound of  $\sqrt{\alpha_{\text{GB}}} \lesssim 1$  km for massless sGB using O1-O3 binaries. However, we note a sign error in the non-GR dephasing term of the waveform model used by (at least) [24].
- [91] B. Shiralilou, T. Hinderer, S. M. Nissanke, N. Ortiz, and H. Witek, *Classical Quantum Gravity* **39**, 035002 (2022).
- [92] B. P. Abbott *et al.* (KAGRA, LIGO Scientific, and Virgo Collaborations), *Living Rev. Relativity* **19**, 1 (2016).
- [93] M. Punturo *et al.*, *Classical Quantum Gravity* **27**, 194002 (2010).
- [94] S. Dwyer, D. Sigg, S. W. Ballmer, L. Barsotti, N. Mavalvala, and M. Evans, *Phys. Rev. D* **91**, 082001 (2015).
- [95] P. Amaro-Seoane *et al.* (LISA Collaboration), [arXiv:1702.00786](https://arxiv.org/abs/1702.00786).
- [96] S. Sato *et al.*, *J. Phys. Conf. Ser.* **840**, 012010 (2017).
- [97] J. Luo *et al.* (TianQin Collaboration), *Classical Quantum Gravity* **33**, 035010 (2016).
- [98] W.-R. Hu and Y.-L. Wu, *Natl. Sci. Rev.* **4**, 685 (2017).
- [99] S. Barsanti, A. Maselli, T. P. Sotiriou, and L. Gualtieri, *Phys. Rev. Lett.* **131**, 051401 (2023).